Proceedings of the 4th International Congress APMAS2014, April 24-27, 2014, Fethiye, Turkey

Electrical Conductivity of Boron Oxide-Doped Yttria-Stabilized Cubic Zirconia (8YSZ)

B. Aktas[a,*] and S. Tekeli[b]

[a]Harran University, Engineering Faculty, Mechanical Engineering Department, 63300, Sanliurfa, Turkey

[b]Gazi University, Technology Faculty, Metallurgical and Materials Engineering Department, 06500, Ankara, Turkey

The effect of B_2O_3 addition on the electrical conductivity of 8 mol% yttria-stabilized cubic zirconia (8YSZ) was investigated by analyzing the impedance spectra of 0–10 wt.% B_2O_3-doped 8YSZ powders prepared via a colloidal process. The doped powders were then pelletized under a pressure of 200 MPa, and then sintered at 1400 °C for 10 h. Measurements of the electrical conductivity of the sintered specimens within a frequency range of 100 mHz–13 MHz, and temperature range of 300–800 °C, revealed an increase in conductivity with increasing temperature. Furthermore, the grain interior, grain boundary and total conductivity of 8YSZ were found to be enhanced by the addition of 1 wt.% B_2O_3. This is attributed to the lattice distortion created by the addition of B^{3+} cations to the 8YSZ lattice, which leads to an increase in the concentration of oxygen vacancies, thus ultimately resulting in an enhanced electrical conductivity.

DOI: 10.12693/APhysPolA.127.1380

PACS: 81.05.Je, 81.20.Ev, 82.47.Ed

1. Introduction

The high ionic conductivity and good stability of yttria-stabilized cubic zirconia (8YSZ) has seen it widely used as an electrolyte material for solid oxide fuel cells (SOFCs), oxygen sensors, and thermal barriers. The addition of Y_2O_3 in solid solution helps to stabilize the fluorite structure of zirconia, thereby increasing its oxygen vacancy concentration. At high temperatures, however, the yttrium ions (3+) are replaced by zirconium ions (4+), creating many lattice vacancies in the process, in order to ensure electrical neutrality. These vacancies, in turn, provide a means for the transportation of oxygen ions through the material under an electrochemical potential at elevated temperatures [1, 2]. Accordingly, there have already been studies into the composition, structure, and conductivity of 8YSZ [3, 4]. In more recent years, the conductivity of ZrO_2 doped with trivalent oxides, such as Sc_2O_3, Yb_2O_3, Dy_2O_3 and Er_2O_3, has been investigated with a view to further improving the ionic conductivity; these results indicating that such additives do indeed increase conductivity [5–7].

Boron oxide (B_2O_3) formed by the thermal fusion of boric acid (H_3BO_3) is amorphous in form, and represents an excellent network former. Moreover, boron oxides offer the advantage of a low coefficient of thermal expansion and high refractive index, and as such have been widely used in glass ceramics [8]. More recently, several researchers have investigated the effect of B_2O_3 addition on the electrical conductivity of ceramic materials. For instance, Tawichai *et al.* have studied its effect on a $Li_{1.5}Al_{0.5}Ge_{1.5}(PO_4)_3$ glass ceramic, finding that the conductivity is increased with the addition of 0.05 wt.% B_2O_3[9]. In another study, the phase transition and electrical properties of $Ba(Ti_{0.9}Sn_{0.1})O_3$ ceramics with B_2O_3 added were investigated, and it was reported that the densification and dielectric properties were improved by the addition of a small amount of B_2O_3 [10].

With this in mind, the objective of this study is to determine the effect of B_2O_3 addition on the ionic conductivity of 8YSZ at low temperatures. The selection of B_2O_3 as a dopant for 8YSZ was based on the significant mismatch between the ionic radii of ZrO_2 and B_2O_3, as well as the fact that their valences are nearly equal. We therefore herein present an analysis of the influence of B_2O_3 addition on the electrical conductivity and microstructure of 8YSZ through impedance spectroscopy and SEM, respectively.

2. Experimental materials and procedure

In this study, 0.3 μm yttria-stabilized cubic zirconia (8YSZ) (Tosoh, Japan) and a 0.75 μm B_2O_3 powder (US Research Nanomaterials, Inc., USA) were used as the matrix material and additive, respectively.

Specimens for microstructural and electrical conductivity analysis were produced by means of colloidal processing. The subsequent doping process was carried out in a plastic container by mixing up to 10 wt.% B_2O_3 with 8YSZ powder, zirconia balls, and ethanol. Mechanical mixing was performed using a "speks" type mixer at a speed of 200 rpm for 12 h, the resulting slurries being allowed to dry naturally by leaving the lid open for 24 h. After drying, the agglomerated powders were ball-milled for 10 min. in order to break up any agglomerates and obtain a good dispersion. These ball-milled powders were passed through a 60 μm sieve, and then pelletized under a pressure of 200 MPa using a single-axis die (radius 10 mm, height 4 mm). The inner surface of this steel

*corresponding author; e-mail: baktas@harran.edu.tr

die was cleaned after each pressing process, and stearic acid was applied to the sidewalls as a lubricant.

The pressed pellets were sintered in a box type furnace at 1400 °C for 10 h under normal atmospheric conditions, with a heating and cooling rate of 5 °C/min. The surface of the sintered specimens was ground and polished using normal metallographic methods, and then thermally etched in the same furnace for 1 h, at a temperature 50 °C below the sintering temperature. The microstructure of the sintered specimens was then analyzed using scanning electron microscopy (SEM, Jeol JSM-6060LV). The corresponding grain sizes were measured using the mean linear intercept method.

Electrical conductivity measurements were performed on sintered pellets measuring 10 mm in diameter and 3 mm in thickness. Both surfaces of these pellets were first slightly polished using abrasive paper, and then electrical connections were drawn by applying platinum paste to both surfaces. The specimens were all dried in an oven at 100 °C to eliminate any excess solvent, and then annealed at 800 °C for 30 min to prevent excessive shrinkage of the platinum electrodes. The temperature dependence of electrical conductivity was measured using a frequency response analyzer (Solartron, Model 1260) within a frequency range of 100 mHz to 13 MHz. All measurements were performed in air, with the temperature ranging from 300 to 800 °C at intervals of 100 °C. The AC impedance diagrams obtained were analyzed using ZView software.

3. Results and discussion

SEM micrographs of 8YSZ in a pure state, and with added B_2O_3, are shown in Fig. 1. As can be seen from this, both the undoped and B_2O_3-doped 8YSZ samples have a coarse-grained microstructure, and coaxial polygonal grains (Fig. 1a–1d). More interesting, however, is the appearance of pores at the grain boundaries of 8YSZ at 5 and 10 wt.% B_2O_3 addition (Fig. 1c and 1d). Since it is known that B_2O_3 can be melted at a relatively low temperature ($\sim$ 450 °C), it is entirely possible that liquid-phase B_2O_3 may have formed at the grain boundaries [10]. If so, then this phase would have evaporated during sintering, the loss of B_2O_3 by evaporation providing an explanation for these grain boundary pores. Furthermore, an overdoping of B_2O_3 (5–10 wt.%) would be expected to cause a higher porosity due to the formation of a glass phase at the grain boundaries. Using a mean linear intercept method, the grain sizes of the undoped and 1, 5, and 10 wt.% B_2O_3-doped 8YSZ samples, are found to be 3.11, 2.8, 3.73, and 5.09 μm, respectively. Thus, increasing the B_2O_3 addition accelerates grain growth after sintering at 1400 °C for 10 h, most likely due to the formation of a liquid phase during sintering. Similar grain growth with B_2O_3 addition has been reported in the literature for $BaTiO_3$ and $Ba_{0.7}Sr_{0.3}TiO_3$ ceramics, with high B_2O_3 additions causing grain growth with pores due to a precipitation mechanism in the liquid phase present during sintering [11, 12].

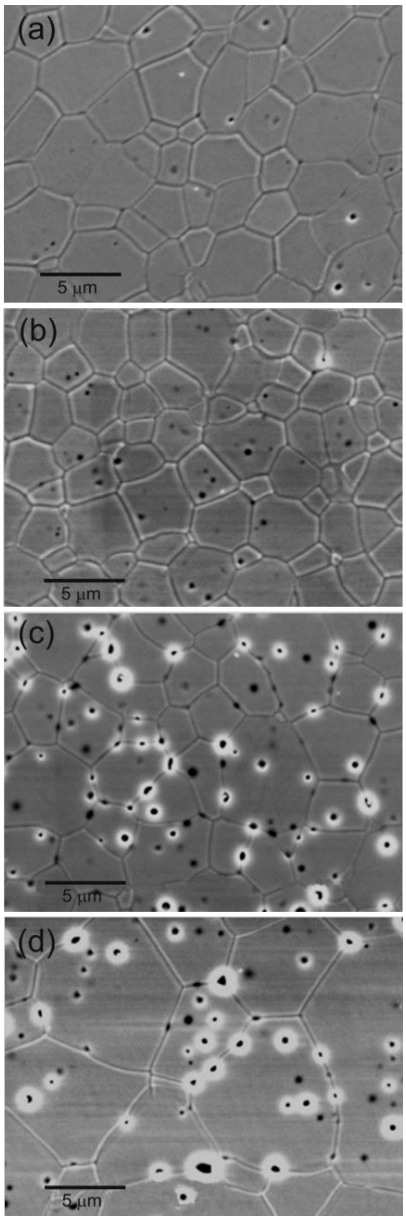

Fig. 1. SEM micrographs of 8YSZ specimens sintered at 1400 °C for 10 h with (a) 0, (b) 1, (c) 5, and (d) 10 wt.% B_2O_3 doping.

Figure 2 demonstrates the change in impedance for the grain interior and grain boundary as a function of dopant concentration. As can be seen from these curves, three arcs are clearly evident at a test temperature of 300 °C for both high and low frequencies (Fig. 2a–2d). The first and second of these arcs represents the grain interior and grain boundary resistance, respectively; while the sum of the two arcs gives the total resistance. Thus, the grain boundary resistance (R_{gb}) of 8YSZ is clearly reduced by the addition of 1 wt.% B_2O_3, the lower value indicating the presence of an electrically conductive phase at the grain boundary. Furthermore, the grain interior resistance (R_{gi}) of a 1 wt.% B_2O_3-doped 8YSZ sample is

also lower than that of undoped 8YSZ. The grain interior (σ_{gi}) and grain boundary (σ_{gb}) conductivities were calculated by the following equation:

$$\sigma_{gi} = \frac{1}{R_{gi}} \frac{L}{A}, \qquad \sigma_{gb} = \frac{1}{R_{gb}} \frac{L}{A}, \tag{1}$$

where R_{gi} is the grain interior resistance, R_{gb} is the grain boundary resistance, and L and A are the thickness and cross-sectional area of the specimen, respectively.

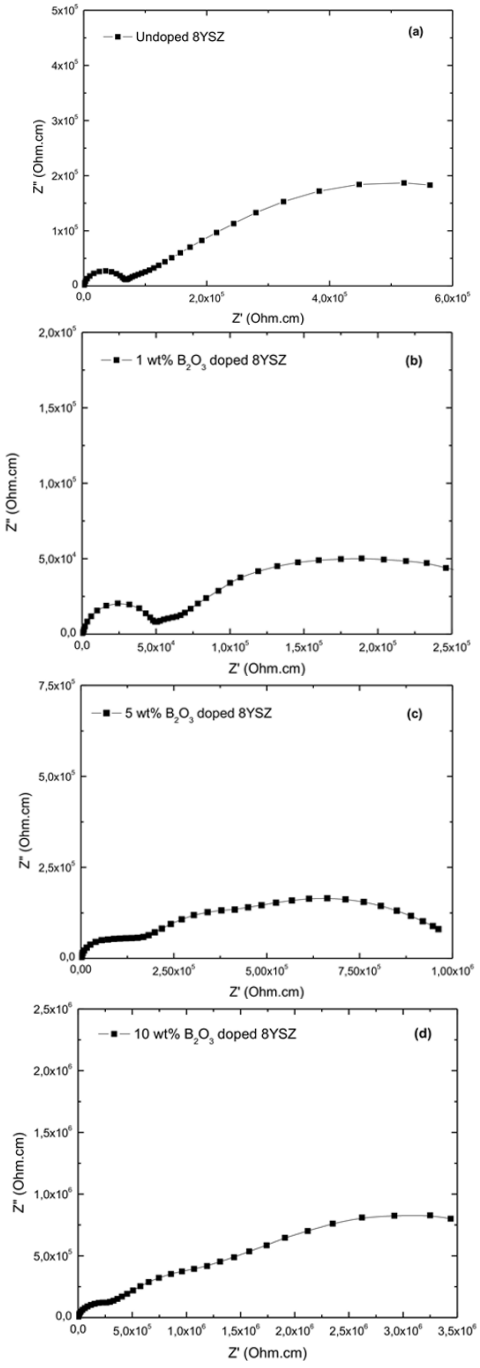

Fig. 2. AC impedance spectroscopy diagrams of 8YSZ specimens at 300 °C with (a) 0, (b) 1, (c) 5, and (d) 10 wt.% B_2O_3-doping.

The effect of B_2O_3 addition on the grain interior (σ_{gi}) and grain boundary conductivity (σ_{gb}) of 8YSZ at 300 °C is presented in Fig. 3. Here, both σ_{gi} and σ_{gb} are again increased with 1 wt.% B_2O_3 addition; the dissolved B^{3+} cations distorting the crystal lattice of 8YSZ, thereby causing an increase in the concentration of oxygen vacancies that increases the grain interior, grain boundary and total conductivity. In principle, both di- and trivalent dopants are capable of introducing oxygen vacancies into a zirconia crystal lattice [13]. However, the addition of 5 and 10 wt.% of B_2O_3 is shown to actually reduce the grain interior, grain boundary, and total conductivity values at 300 °C. It is possible that with increasing B_2O_3 content, the defects associated with oxygen vacancies clustered in the grain interior may reduce the mobility of oxygen ions. This decrease in conductivity may then result in the vacancies becoming more regular by interaction with defect pairs, thereby blocking each other. Thus, an improved ionic conductivity is only evident when a small amount of B_2O_3 is added (1 wt.%), due to lattice distortion in the 8YSZ, and the formation of a conductive secondary phase at the grain boundaries.

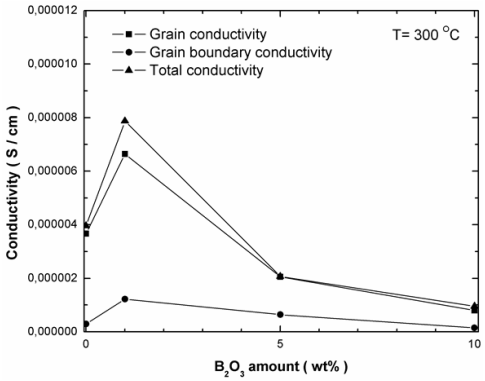

Fig. 3. The effect of B_2O_3 content on the conductivity of 8YSZ at 300 °C.

The grain interior and grain boundary activation energies for undoped and B_2O_3- doped 8YSZ samples were calculated using the Arrhenius equation:

$$\sigma = \frac{\sigma_0}{T} \exp\left(-\frac{E_a}{k_B T}\right), \tag{2}$$

where T is the absolute temperature, σ_0 is a pre-exponential factor, and E_a and k_B are the activation energy and Boltzmann constant, respectively.

Figure 4 shows the grain interior and the grain boundary activation energies (E_a) for the undoped and B_2O_3-doped 8YSZ samples. From this, the E_a values of the undoped and 1, 5, and 10 wt.% B_2O_3-doped 8YSZ samples were calculated as 1.15, 1.07, 1.09, and 1.13 eV, respectively (Fig. 4a). We can see from this, that the grain interior activation energy in B_2O_3-doped 8YSZ is lower than that of undoped 8YSZ, suggesting that the transfer of ions in the grain interior is aided by a 1 wt.% B_2O_3 addition.The grain boundary activation energy for un-

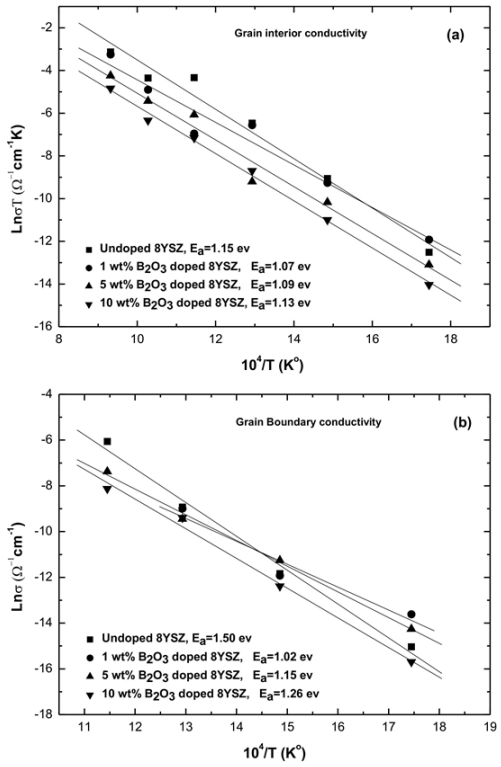

Fig. 4. Change in activation energies of undoped and B_2O_3-doped 8YSZ specimens for the (a) grain interior and (b) grain boundary conductivity.

doped 8YSZ was calculated as 1.50 eV; and for the 1, 5, and 10 wt.% B_2O_3-doped 8YSZ samples as 1.02, 1.15, and 1.26 eV, respectively (Fig. 4b). The lower values obtained for the B_2O_3-doped 8YSZ specimens mean that ion transfer at the grain boundary is indeed easier than that of undoped 8YSZ, with the low grain boundary activation energy also indicative of an electrical conductor. This decrease in the grain boundary activation energy is attributable to the presence of B_2O_3 as a secondary phase at the grain boundaries and triple points of 8YSZ, creating an increase in B^{3+} charge carrier ions with increasing temperature.

4. Conclusions

This study has shown that the addition of B_2O_3 to 8YSZ causes an increase in grain size after sintering due to the formation of a liquid phase at the grain boundaries. An increase observed in the grain interior and grain boundary conductivity of 8YSZ at 300 °C with the addition of 1 wt.% B_2O_3 is attributed to the lattice distortion caused by the addition of B^{3+} cations into the 8YSZ lattice. This leads to an increase in the concentration of oxygen vacancies in 8YSZ, thus resulting in an enhancement of its electrical conductivity. On the basis of the activation energy results, the grain interior and grain boundary ion transport is clearly improved in the case of 1 wt.% B_2O_3-doped 8YSZ, when compared with its undoped state, which is considered to be related to the increased oxygen vacancies. Thus, the grain interior and the grain boundary activation energy of 8YSZ is reduced by the addition of 1 wt.% B_2O_3.

Acknowledgments

This work has been supported by HUBAK (the scientific research projects commission of Harran University, Sanliurfa, TURKEY) under project number K14005. The authors are grateful to the scientific research projects commission of Harran University for financial support, and Gazi University for the provision of laboratory facilities.

References

[1] M.J. Verkerk, A.J.A. Winnubst, A.J. Burggraaf, *J. Mater. Sci.* **17**, 3113 (1982).

[2] M. Miyayama, H. Yanagida, A. Asada, *Am. Ceram. Soc. Bull.* **64**, 660 (1985).

[3] B. Aktaş, *High Temp. Mater. Proc.* **32**, 551 (2013).

[4] T.L. Wen, D. Wang, M. Chen, H. Tu, Z. Lu, Z. Zhang, H. Nie, W. Huang, *Solid State Ionics* **148**, 513 (2002).

[5] Y. Li, J. Gong, Z. Tang, Z. Zhang, *J. Chin. Ceram. Soc.* **25**, 705 (1997).

[6] Z. Lv, R. Guo, P. Yao, F. Dai, *Mater. Des.* **28**, 1399 (2007).

[7] B. Aktas, S. Tekeli, M. Kucuktuvek, *J. Mater. Eng. Perform.* **23**, 349 (2014).

[8] S. Koçyiğit, Ö. Gökmen, S. Temel, A. Aytimur, İ. Uslu, S.H. Bayari, *Ceram. Int.* **39**, 7767 (2013).

[9] H.S. Jadhav, M.S. Cho, R.S. Kalubarme, J.S. Lee, K.N. Jung, K.H. Shin, C.J. Park, *J. Power Sources* **241**, 502 (2013).

[10] N. Tawichai, U. Intatha, S. Eitssayeam, K. Pengpat, G. Rujijanagul, T. Tunkasiri, *Phase Transit.* **83**, 55 (2010).

[11] H. Erkalfa, B. Yuksel, T.O. Ozkan, *Key Eng. Mater.* **264-268**, 1333 (2004).

[12] S.M. Rhim, H. Bak, S. Hong, O.K. Kim, *J. Am. Ceram. Soc.* **83**, 3009 (2000).

[13] M.B. Ricoult, M. Badding, Y. Thibault, *Adv. El. Electroch. Ceram.* **179**, Wiley USA, pp. 173, 2012.